Title

Atrophy in behavioural variant frontotemporal dementia spans multiple large-scale prefrontal and temporal networks.

Journal

Brain, 146(11)

Authors

Eldaief, Mark
Brickhouse, Michael
Katsumi, Yuta
et al.

Publication Date

2023-11-02

DOI

10.1093/brain/awad167

Peer reviewed

BRAIN
ORIGINAL ARTICLE

Atrophy in behavioural variant frontotemporal dementia spans multiple large-scale prefrontal and temporal networks

Mark C. Eldaief,[1,2,3,4,†] Michael Brickhouse,[1,†] Yuta Katsumi,[1] Howard Rosen,[5] Nicole Carvalho,[1] Alexandra Touroutoglou[1,2,†] and Bradford C. Dickerson[1,2,3†]

[†]These authors contributed equally to this work.

See Ducharme (https://doi.org/10.1093/brain/awad320) for a scientific commentary on this article.

The identification of a neurodegenerative disorder's distributed pattern of atrophy—or atrophy 'signature'—can lend insights into the cortical networks that degenerate in individuals with specific constellations of symptoms. In addition, this signature can be used as a biomarker to support early diagnoses and to potentially reveal pathological changes associated with said disorder. Here, we characterized the cortical atrophy signature of behavioural variant frontotemporal dementia (bvFTD).

We used a data-driven approach to estimate cortical thickness using surface-based analyses in two independent, sporadic bvFTD samples ($n = 30$ and $n = 71$, total $n = 101$), using age- and gender-matched cognitively and behaviourally normal individuals. We found highly similar patterns of cortical atrophy across the two independent samples, supporting the reliability of our bvFTD signature. Next, we investigated whether our bvFTD signature targets specific large-scale cortical networks, as is the case for other neurodegenerative disorders. We specifically asked whether the bvFTD signature topographically overlaps with the salience network, as previous reports have suggested. We hypothesized that because phenotypic presentations of bvFTD are diverse, this would not be the case, and that the signature would cross canonical network boundaries. Consistent with our hypothesis, the bvFTD signature spanned rostral portions of multiple networks, including the default mode, limbic, frontoparietal control and salience networks. We then tested whether the signature comprised multiple anatomical subtypes, which themselves overlapped with specific networks. To explore this, we performed a hierarchical clustering analysis. This yielded three clusters, only one of which extensively overlapped with a canonical network (the limbic network).

Taken together, these findings argue against the hypothesis that the salience network is preferentially affected in bvFTD, but rather suggest that—at least in patients who meet diagnostic criteria for the full-blown syndrome—neurodegeneration in bvFTD encompasses a distributed set of prefrontal, insular and anterior temporal nodes of multiple large-scale brain networks, in keeping with the phenotypic diversity of this disorder.

1 Frontotemporal Disorders Unit and Alzheimer's Disease Research Center, Department of Neurology, Massachusetts General Hospital and Harvard Medical School, Boston, MA 02114, USA
2 Athinoula A. Martinos Center for Biomedical Imaging, Massachusetts General Hospital, Charlestown, MA 02129, USA
3 Department of Psychiatry, Massachusetts General Hospital and Harvard Medical School, Boston, MA 02114, USA
4 Center for Brain Sciences, Harvard University, Cambridge, MA 02138, USA
5 Department of Neurology, Memory and Aging Center, University of California, San Francisco, San Francisco, CA 94158, USA

Received November 01, 2022. Revised April 10, 2023. Accepted April 16, 2023. Advance access publication May 18, 2023

Correspondence to: Brad Dickerson, MD
MGH Frontotemporal Disorders Unit, Department of Neurology
Massachusetts General Hospital
149 13th Street, Suite 10.004 Charlestown, MA 02129, USA
E-mail: brad.dickerson@mgh.harvard.edu

Keywords: behavioural variant frontotemporal dementia (bvTD); salience network; control network; default-mode network; limbic network

Introduction

When neurodegenerative diseases present as canonical clinical syndromes, patients typically exhibit characteristic patterns of cortical atrophy, or atrophy 'signatures'.[1-3] Delineation of these signatures can offer valuable insights into the large-scale brain networks that are selectively vulnerable in patients presenting with these symptom constellations. This information can be used to support diagnosis, prognostication and to guide novel therapeutic interventions.[2] Although robust work has demonstrated the atrophy patterns typically associated with behavioural variant frontotemporal dementia (bvFTD), little work has been done to examine the reliability of a bvFTD cortical atrophy signature across samples, and the overlap of the full signature with specific large-scale networks of the brain.

The latter issue is of particular importance, as patients presenting with canonical neurodegenerative clinical syndromes exhibit neurodegeneration that preferentially targets key nodes of large-scale neural networks.[3-11] For example, in typical presentations of Alzheimer's disease (AD), hippocampal-parietal nodes of the default mode network (DMN) are preferentially involved, and these patients present with the characteristic clinical symptom of memory loss.[7,12-14] Moreover, other large-scale brain networks are vulnerable to atypical presentations of AD—including preferential degeneration of the language network in logopenic variant primary progressive aphasia and specific degeneration of extrastriate visual and parietal networks in the posterior cortical atrophy syndrome.[15] Based on prior reports, bvFTD is thought to preferentially target the salience network, which is anchored by the frontoinsula and the dorsal anterior midcingulate cortex.[4,8,9,16,17] In this framework, bvFTD is primarily conceptualized as a disorder of processing salient interoceptive or external stimuli.[16,17]

However, while bvFTD is often discussed as a unitary clinico-anatomical disorder, bvFTD patients exhibit considerable clinical phenotypic[18,19] and anatomic heterogeneity.[20] Given the heterogeneity of the cognitive, affective, social, behavioural and neuroanatomical features of bvFTD, we hypothesized that in a typical sample of bvFTD patients, the signature would extend beyond the borders of the salience network to include other major prefrontal and anterior temporal association networks. That is, given that bvFTD patients often exhibit different topographical patterns of frontotemporal atrophy on clinical imaging, it is likely that a bvFTD atrophy signature would not be relegated to a single network. Similarly, because typical bvFTD patients exhibit symptoms that are referrable to more than one network, we hypothesized that the signature would cross network boundaries. To investigate this, we derived a data-driven bvFTD cortical atrophy signature as we previously did for AD.[1] Specifically, we estimated cortical thickness using surface-based analyses of structural MRI data, as described in our previous studies,[1] in two independent bvFTD patient samples: a Massachusetts General Hospital (MGH) FTD Unit sample ($n = 30$) and a sample derived from the Frontotemporal Lobar Degeneration Neuroimaging Initiative (FTLD-NI) ($n = 71$), and compared cortical thickness across the entire cortical mantle—not constrained to specific regions of interest—in these cohorts to age and gender-matched controls. This allowed us to examine the reproducibility of atrophy patterns in bvFTD and to investigate whether there is a distinct signature in patients with this clinical syndrome. We hypothesized that the localization of atrophy would extend beyond the boundaries of the canonical salience network to involve three other large-scale networks: (i) the limbic (also know as semantic appraisal) network, anchored in rostromedial ventral prefrontal (i.e. ventromedial prefrontal and medial orbitofrontal) cortex and the anterior temporal lobe (i.e. the temporal pole); (ii) anterior portions of the DMN, including rostral portions of the anterior cingulate, dorsomedial prefrontal cortex and middle temporal gyrus; and (iii) the frontoparietal (also known as executive control) network (FPN), including dorsolateral prefrontal cortex and portions of dorsomedial prefrontal cortex. This was assessed by comparing the topography of the data-driven bvFTD signature to that of seven major large-scale networks.[21] We then explored the between-subjects clustering of this signature into anatomic subtypes.

Materials and methods

Participants

Data used in this study were obtained from two independent cohorts. The MGH bvFTD Cohort included 30 patients who were participants in the ongoing Massachusetts General Hospital Frontotemporal Disorders Unit Longitudinal Cohort. Participants underwent a comprehensive clinical evaluation as previously described in our prior studies.[22,23] We performed a multidisciplinary assessment including a structured interview by a behavioural neurologist or neuropsychiatrist specializing in dementia. This assessment included measures of cognition, mood/behaviour, sensorimotor function and daily activities; a neurological examination, including office-based cognitive testing and a brief psychiatric interview; as well as a neuropsychological assessment. A clinician also performed a structured interview with a care partner, augmented with standard questionnaires. The protocol also included the National Alzheimer's Coordinating Center (NACC) Uniform Data Set (using version 2.0 previously and currently version 3.0) and supplementary measures. In addition, after the clinical assessment was performed and preliminary diagnostic formulation is rendered, an MRI scan with T_1- and T_2-weighted sequences was inspected visually by a behavioural neurologist or neuropsychiatrist—independently of any quantitative analysis—to examine for predicted regional atrophy and the presence of other lesions (in this case to determine whether the patient meets clinical diagnostic criteria for probable bvFTD).

Cases selected for this study were diagnosed with sporadic probable bvFTD according to consensus guidelines.[24] Visual inspection of clinical MRIs in these individuals revealed cortical atrophy that was most prominent in the frontal and/or anterior temporal lobes and ruled out other causes of focal brain damage. All patients were right-handed, and all were native English speakers. All patients and their care partners denied a pre-existing psychiatric disorder, other neurological disorder or developmental cognitive disorder. All patients and their care partners gave written informed consent in accordance with guidelines established by the Mass General Brigham Healthcare System Institutional Review Boards, which govern human subjects research at MGH.

The second cohort included 71 participants in the FTLD-NI (4rtni-ftldni.ini.usc.edu), a multisite observational frontotemporal lobar degeneration (FTLD) natural history and biomarker study involving 18 months of longitudinal follow-up with neuropsychiatric, neuropsychological, neuroimaging, blood and CSF examinations. Participants in this study were recruited at the University of California, San Francisco (UCSF) Memory and Aging Center, Mayo Clinic (Rochester, MN), or MGH; for the present analysis, cases from MGH were excluded. All participants received a standard clinical evaluation that included a comprehensive neurological history, physical and neurological examinations, structured caregiver interviews, neuroimaging and neuropsychological testing. Patient diagnoses were established by consensus by a multidisciplinary team applying consensus diagnostic criteria for bvFTD.[24] Of note, the FTLD-NI cohort was not matched to their controls on the demographic factor of years of education (Table 1). The UCSF, Mayo Clinic and MGB Institutional Review Boards for human research approved the study. Informed consent was obtained from all participants or their assigned surrogate decision-makers.

All the cases in both cohorts were tested for mutations in *MAPT*, *GRN* and *c9orf72*; the cases included in this report were all negative for those mutations. Clinical and demographic characteristics of the two cohorts are depicted in Table 1.

Structural MRI data acquisition and analysis

MRI data for the MGH cohort were acquired with a Siemens Trio 3.0 T scanner (Siemens Medical Systems). Sequences acquired included a high resolution T_1-weighted MPRAGE (repetition time = 2.3 s, echo time = 2.98 ms, field of view = 256 mm, flip angle = 7°, 192 sagittal 1 mm-thick slices, matrix 240 × 256). A FLAIR sequence was also included for the purpose of ruling out non-degenerative neurological diseases, which may have been contributing to patients' clinical syndromes.

For the FTLD-NI cohort, the two sites used different scanners with harmonized protocols. At UCSF, whole-brain structural MRIs were acquired on a 3 T Siemens Tim Trio using volumetric magnetization-prepared rapid gradient echo (MPRAGE) sequence (coronal slice orientation; slice thickness 1.0 mm; in-plane resolution 1.0 × 1.0 mm; matrix 240 × 256; repetition time = 2.3 ms; echo time = 3 ms; inversion time = 900 ms; flip angle 9°). At the Mayo Clinic, structural MRI was acquired on a 3 T General Electric MRI (model DISCOVERY MR750) with the following parameters: coronal slice orientation; slice thickness 1.2 mm; in-plane resolution 1.0156 × 1.0156 mm; matrix 256 × 256; repetition time = 7.3 ms; echo time = 3 ms; inversion time = 900 ms; flip angle = 8°.

Each subject's T_1-weighted MPRAGE MRI scan was analysed using Freesurfer version 6 to estimate cortical thickness (http://surfer.nmr.mgh.harvard.edu). Each subject's scan was manually checked for errors in segmentation leading to errors in white matter or pial surface identification, and manual edits were made. Cortical thickness was estimated in both samples using FreeSurfer's standard reconstruction and analysis pipeline. Cortical thickness in these samples were then compared to that measured in two groups of age- and gender-matched controls ($n = 60$ and $n = 133$, respectively) by smoothing at 15 mm full-width at half-maximum on the surface running a surface vertex-wise two class general linear model analysis. Maps depicting where cortical thickness was statistically significantly different in the standard FreeSurfer general linear model (*glmfit*) between patients and controls in the MGH discovery sample were generated (*sig* maps) and overlaid with effect size maps (*gamma*), which indicate the magnitude of group differences in cortical thickness at each vertex in tenths of millimetres. Since the FTLD-NI replication sample was larger, which influences the statistical significance of effects, the effect size measure was used to threshold both maps at 0.3 mm. That is, only cortical regions that were at least 0.3 mm thinner in patients than controls contributed to the bvFTD signature maps.

Calculating overlap of gamma maps with established large-scale networks

To estimate individual network atrophy in bvFTD, we then compared the resultant cortical thickness difference maps to the

Table 1 Characteristics of patient and control cohorts

	MGH cohort		P-value	FTLD-NI cohort		P-value
	bvFTD patients ($n = 30$)	Healthy controls ($n = 60$)		bvFTD patients ($n = 71$)	Healthy controls ($n = 133$)	
Mean age, years	62.0 (8.4)	62.8 (9.7)	0.90	61.6 (6.5)[a]	63.2 (7.3)	0.12
Gender	17 M, 13 F	34 M, 26 F	–	45 M, 26 F	58 M, 75 F	–
Mean years education	15.8 (2.5)	16.1 (2.6)[b]	0.37	15.5 (3.3)[a]	17.3 (1.9)[b]	<0.001*
CDR global rating (number subjects with 0.5/1)	18/12	–	–	18/34[a]	–	–
Mean CDR SOB	3.9 (1.9)	–	–	6.1 (3.1)[a]	–	–
Mean CDR Behaviour	1.4 (0.5)	–	–	1.4 (0.8)[a]	–	–
Mean CDR + FTLD SOB	5.5 (2.2)	–	–	8.1 (3.9)[a]	–	–

Values are presented as mean (SD). bvFTD = behavioural variant frontotemporal dementia; CDR SOB = Clinical Dementia Rating Scale Sum of Boxes; F = female; FTLD-NI = Frontotemporal Lobar Degeneration Neuroimaging Initiative; M = male; MGH = Massachusetts General Hospital.

[a]One missing value.

[b]Seven missing values.

*Significant *P*-value.

topography of seven large-scale cortical networks derived from the Yeo *et al.*[21] parcellation. We binarized the gamma maps at a thickness difference threshold of 0.3 mm; each cortical vertex where the bvFTD group is at minimum 0.3 mm thinner than the control group is included in this binary map. We then overlaid this map on the cortical surface along with the Yeo network parcellation and calculated the percentage of vertices where each network overlapped with the binarized bvFTD signature maps.

Hierarchical clustering analysis

Given that a randomly selected cohort of bvFTD patients may exhibit heterogeneous atrophy patterns,[20] we next evaluated whether our bvFTD signature comprised distinct anatomical subtypes. If true, one or more of these subtypes might overlap more specifically with an established network (such as the salience network) even if the larger pooled group did not. To explore this possibility, we performed a data-driven hierarchical clustering analysis to identify clusters of patients with similar atrophy maps based on spatial patterns of cortical atrophy in the pooled bvFTD dataset ($n = 101$, containing both samples). We first converted each patient's vertex-wise cortical thickness map to a *W*-score map, which was used to estimate the magnitude of cortical atrophy at each vertex point. This was done in a cohort-specific manner, i.e. MGH patients were compared to maps from MGH controls and FTLD-NI patients were compared to FTLD-NI controls. *W*-scores are analogous to *Z*-scores adjusted for specific covariates of no interest, which in this study were age and gender.[25,26] Calculation of *W*-scores was performed via a vertex-wise multiple regression analysis using cortical thickness data from healthy controls, resulting in whole-cortex beta coefficient maps of age and gender, as well as individual maps of residuals. For each patient at each vertex, a *W*-score was calculated using the following formula:

$$W = \frac{\text{Thickness}_{\text{actual}} - \text{Thickness}_{\text{predicted}}}{\text{SD}_{\text{residuals}}} \quad (1)$$

where $Thickness_{actual}$ = the observed value of cortical thickness for a given patient, $Thickness_{predicted}$ = the predicted value of cortical thickness based on the beta coefficients obtained from healthy control participants of the same age and gender, and $SD_{residuals}$ = the standard deviation of the individual residual maps obtained from healthy controls.

Next, we quantified the extent of spatial similarity between each unique pair of *W*-score maps for the 101 individual bvFTD patients using η^2.[27] η^2 can vary from 0 (no similarity) to 1 (identical) and measures the difference in values at corresponding data-points in a pair of statistical maps, not strictly whether the values vary in similar ways, but can also detect similarities and differences in the maps using information from all data-points.[28] Our approach therefore capitalized on all ~160k vertices in the *fsaverage* template surface space, unlike previous studies of subtype clustering in bvFTD that used a limited set of regions of interest (ROIs) representing a few functional networks[29,30] or a set of ROIs with coarse resolution.[20,31] This procedure yielded a 101×101 matrix where each cell represented the similarity in spatial patterns of cortical atrophy between a given pair of patients. Using the η^2 matrix as input, we performed an agglomerative hierarchical clustering analysis with average-linkage implemented in *scikit-learn* version 0.23.2[32] run in Python version 3.8.5.

Statement of ethics

The protocol used for research with the MGH cohort presented in this paper was approved by the Massachusetts General Hospital/Partners Human Research Committee. All participants gave written informed consent in accordance with guidelines established by the Massachusetts General Hospital/Partners Human Research Committee. The protocol used for research with the FTLDNI cohort was approved by the UCSF, Mayo Clinic and MGB Institutional Review Boards.

Data availability

Study data include structural MRIs derived from the FTLD-NI and MGH datasets. De-identified data from the FTLD-NI dataset can be accessed upon request and after agreeing to the appropriate data terms at the 4-Repeat Tauopathy and Frontotemporal Lobar Neuroimaging Initiatives website at http://4rtni-ftldni.ini.usc.edu. Data from the MGH dataset that support the findings of this study are available from the corresponding author, upon reasonable request.

Results

The bvFTD signature is robustly reproducible across independent cohorts

In both cohorts, prominent cortical atrophy was present in superior frontal gyrus, dorsomedial prefrontal cortex and dorsal and subgenual anterior cingulate cortex, temporal pole, middle temporal gyrus and anterior medial temporal lobe. Orbitofrontal cortex and fronto-insula were more notably atrophic in the MGH sample than in the FTLD-NI sample. The pooled sample shows atrophy in all of these regions. Importantly, visual inspection of the bvFTD signature shows that this signature was remarkably consistent across the two cohorts, even though these cohorts were independently acquired on separate scanners (using harmonized protocols) (Fig. 1).

The bVTD signature involves multiple large-scale networks

Consistent with our hypotheses, the pooled bvFTD signature (averaged across both cohorts) extended well beyond the confines of the salience network. While the signature did include the salience network, it also spanned the limbic (i.e. semantic appraisal) network and rostral portions of the default mode and frontoparietal networks (Fig. 2). We quantitatively assessed the involvement of each large-scale network in the bvFTD signature. To do so, we defined a ROI encompassing the surface area of the entire signature and calculated the percentage of the bvFTD signature that was made up by components of each of the seven major networks (in the Yeo *et al.*[21] seven network parcellation). Of the entire bvFTD signature, 46.3% of the surface area, particularly dorsomedial prefrontal cortex, superior frontal gyrus and middle temporal gyrus, belonged to the DMN. Yeo *et al.*'s 'limbic' (i.e. semantic appraisal) network was second, making up 24.5% of the bvFTD signature, followed by the salience network (14.2%) and the frontoparietal network (13.1%). As expected, the visual, dorsal attention and somatomotor networks each contributed to less than 1% of the signature, as nodes of these networks are all situated posteriorly and caudally.

However, because we sampled atrophy cross-sectionally, and because we did not employ novel machine learning paradigms that can estimate disease stage,[33] it is possible that atrophy may have begun in the salience network in these patients, and that the inclusion of other cortical networks in our signature reflects the spread of atrophy to these systems with disease progression. To explore this

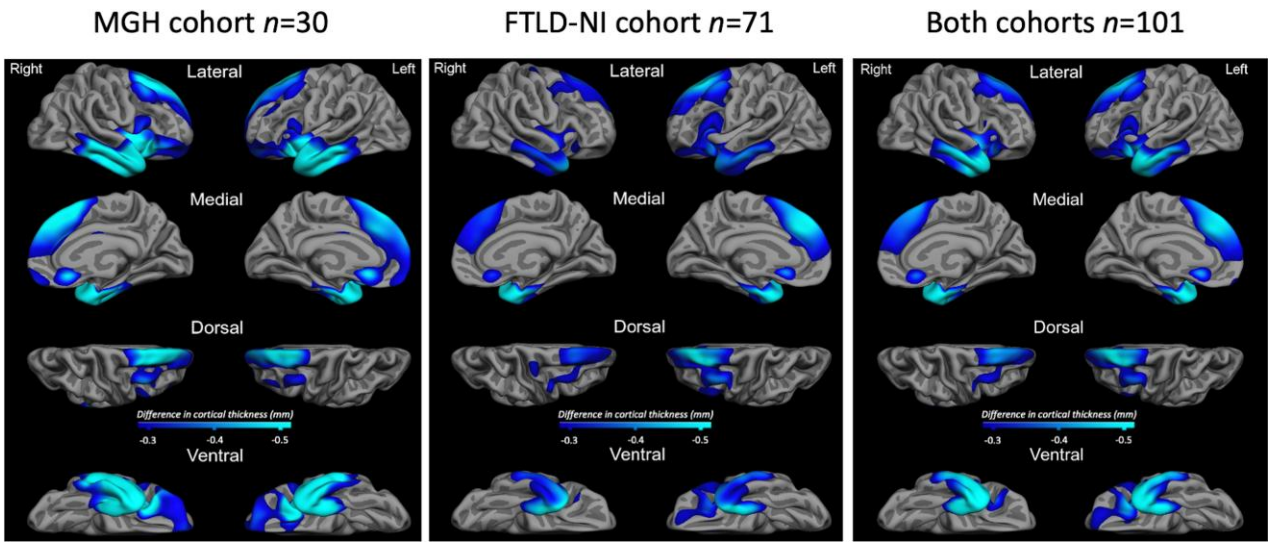

Figure 1 The bvFTD signature is highly similar across two independent cohorts. Gamma maps of cortical atrophy, thresholded so that only regions with at least 0.3 mm or more of atrophy are depicted, show that both cohorts exhibit highly co-localized regional atrophy. Maps are shown for the Massachusetts General Hospital (MGH) cohort (*left*), Frontotemporal Lobar Degeneration Neuroimaging Initiative (FTLD-NI) cohort (*middle*) and as an average of both cohorts (*right*).

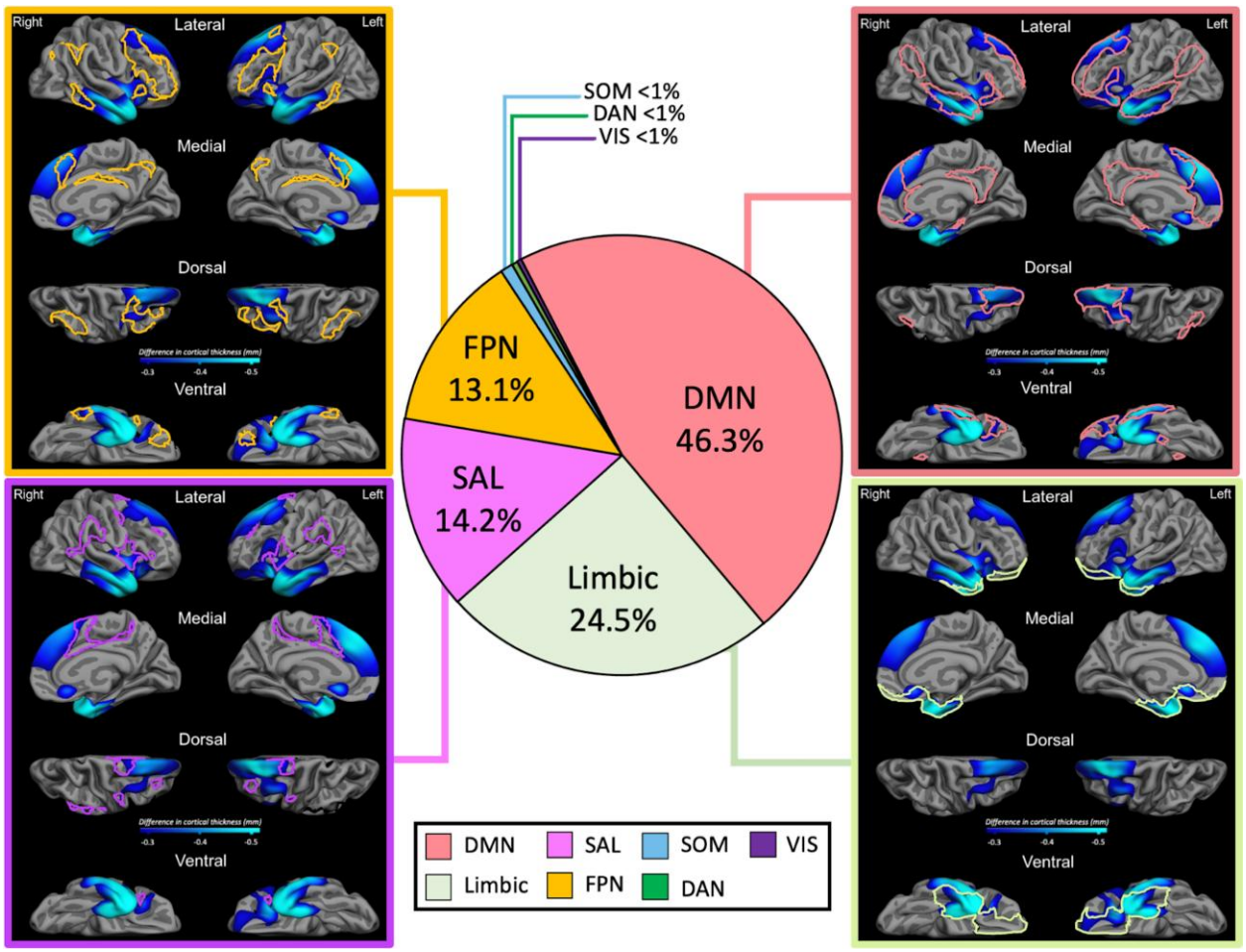

Figure 2 Breakdown of the bvFTD signature by network. *Middle*: Pie chart demonstrating the percentage to which each of the major networks in the Yeo *et al.*[21] parcellation contribute to the pooled bvFTD signature (averaged across cohorts). The default mode network (DMN) contributed the most to the signature, followed by the limbic network, salience network (SAL) and the frontoparietal network (FPN). As expected, the remaining three networks [dorsal attention (DAN), somatomotor (SOM) and visual (VIS)] contributed negligibly to the signature. Pie chart colours recapitulate those used in Yeo *et al.*[21] and a colour key is provided below the pie chart. *Left* and *right* panels display the overlap between the pooled bvFTD signature from Fig. 1 and the four prefrontal/temporal networks. In each case, the boundaries of a given network are outlined in their corresponding colour. Networks highlighted include (*clockwise from top left*): FPN, DMN, limbic and SAL.

possibility, we applied a similar method to characterize atrophy in individual subjects as we used at the group level. That is, we obtained gamma maps of each subject binarized at a cortical thickness of >0.3 mm thinner than the control group. We then examined how many individuals harboured atrophy within the demarcations of the salience network. If the majority of individuals exhibited atrophy in the salience network using this method, this would support the hypothesis that atrophy may have begun there. If, on the other hand, this was not the case, it would support the hypothesis that this network was never affected in a large percentage of patients. The results of this analysis are shown in Supplementary Fig. 1, which depicts the percentage overlap of topographical atrophy across bvFTD patients in each cohort. As can be appreciated in this figure, the majority of individuals did not exhibit atrophy in canonical salience network regions, although there was considerable overlap in portions of the fronto-insular ROI of this network. This supports the notion that atrophy in bvFTD does indeed involve multiple networks, as opposed to spreading from the salience network to these systems with disease progression.

Hierarchical clustering revealed three anatomical subtypes of the bvFTD signature

To investigate the possibility that distinct anatomical signatures were embedded in the pooled sample, and that these signatures might themselves overlap with canonical networks, we performed an agglomerative hierarchical clustering analysis (Fig. 3). The optimal number of clusters was determined to be five based on the variance-ratio criterion, defined as the ratio of between-cluster variance to within-cluster variance. Visual inspection of the mean W-score map as well as individual maps for each cluster revealed that one cluster ($n = 3$) exhibited a widespread pattern of atrophy throughout the cortex. Moreover, another cluster ($n = 20$) showed minimal atrophy for the group as a whole and included patients with relatively mild diffuse or focal atrophy patterns that did not consistently overlap with each other. We therefore only report the remaining three clusters here (Fig. 3C). Based on general anatomical patterns, we refer to these clusters as the 'fronto-temporo-parietal cluster,' the 'fronto-temporal cluster' and the 'anterior temporal-insular cluster.' Only one of these clusters (the anterior temporal-insular cluster) exhibited topographical overlap with a specific canonical network. This cluster topographically resembled the limbic (i.e. semantic appraisal) network. The remaining two clusters overlapped with the DMN and FPN, and to a lesser extent with the salience network.

Discussion

We used a data-driven whole-cortex approach to examine the spatial topography and magnitude of regional cortical atrophy in two

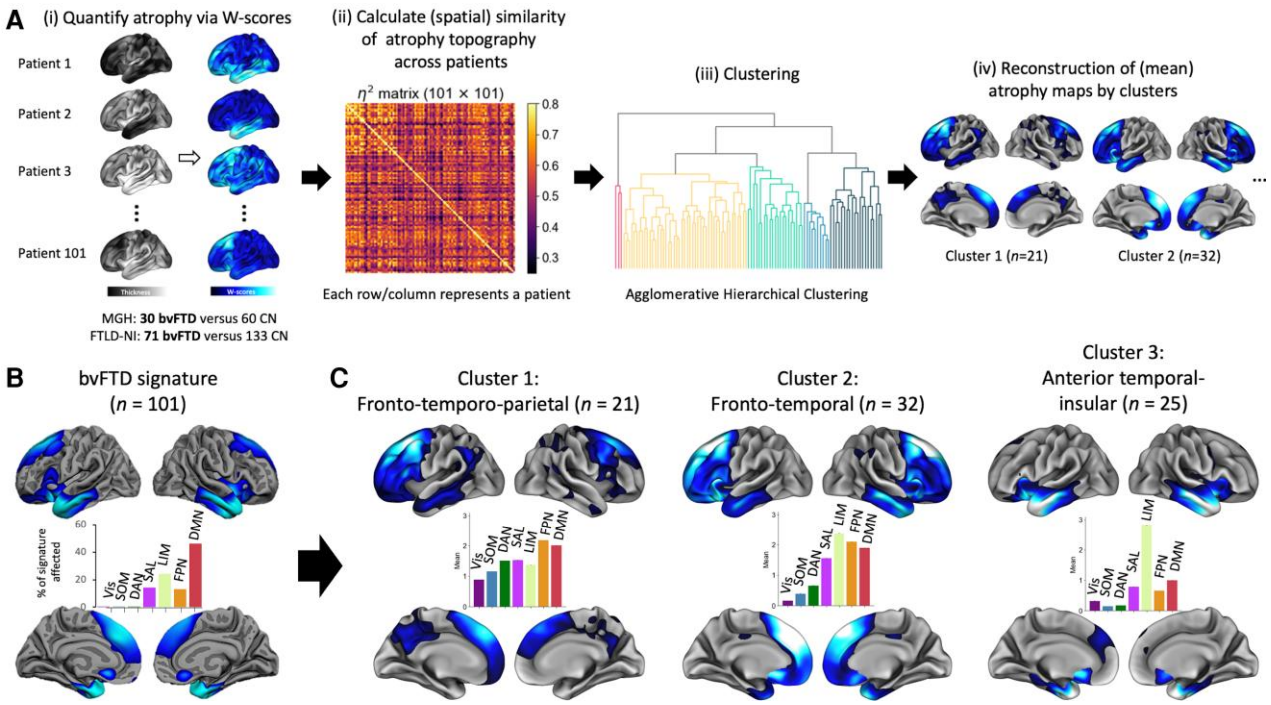

Figure 3 Hierarchical clustering analysis methods and results. The methodology for the hierarchical clustering analysis is shown in **A**. First, each behavioural variant frontotemporal dementia (bvFTD) patient's vertex-wise cortical thickness map was converted to a W-score map. Next, the extent of spatial similarity between each unique pair of W-score maps was calculated for all the bvFTD patients using η^2. This yielded a 101 × 101 matrix, where each cell represented the similarity in spatial patterns of cortical atrophy between a given pair of patients. After this, an agglomerative hierarchical clustering analysis was performed using the η^2 matrix as an input. Coloured vertices on the cortical surface maps represent areas where each group of bvFTD patients showed relatively greater atrophy than amyloid-β– controls at a vertex-wise threshold of $W < -1.5$. Bar graphs depict the percentage of the surface area of the bvFTD signature that falls within the boundaries of each functional network. The pooled bvFTD signature map and % of network overlap is shown in **B**. The three informative clusters derived from the clustering analysis are shown in **C**; i.e. fronto-temporal-parietal, anterior temporal-insular, fronto-temporal. While the anterior temporal-insular cluster showed selective overlap with the limbic (i.e. semantic appraisal) network, the other two clusters did not demonstrate network selectivity. DAN = dorsal attention network; DMN = default mode network; FPN = frontoparietal network; FTLD-NI = Frontotemporal Lobar Degeneration Neuroimaging Initiative; LIM = limbic network; MGH = Massachusetts General Hospital; SAL = salience network; SOM = somatomotor network; VIS = visual network.

independent samples of sporadic bvFTD and found highly reproducible patterns of atrophy across the two cohorts ($n = 101$ patients total) (Fig. 1). We propose this as a 'signature' pattern of atrophy in groups of patients with the bvFTD behavioural-cognitive syndrome, which is typically due to one of the forms of FTLD.

Many of our findings resonate with those demonstrated in prior studies, but we also observed key differences from findings discovered in previous work. For example, despite prior suggestions that prefrontal atrophy is right lateralized in bvFTD,[34] we found relatively symmetrical atrophy across the two hemispheres. With respect to specific frontotemporal cortical regions involved in the bvFTD signature, several prior studies have echoed our findings of atrophy in dorsolateral, dorsomedial and rostral anterior cingulate portions of prefrontal cortex, as well as in anterior temporal and insular cortex[20,29,30,35,36] (Fig. 1). Other studies have identified similar regions when using cortical thinning as a means to differentiate bvFTD from AD.[37-41] Interestingly, two such studies found that preferential thinning of the subgenual cingulate (Brodmann area, BA 25) differentiated bvFTD from AD,[39,40] and we found significant involvement of this region in our signature. This region is hyperactive and hyperconnected in patients with major depressive disorder.[42-45] As such, preferential atrophy of this region could be associated with hedonically driven behavioural symptoms in bvFTD. There were also notable differences between our signature and regional atrophy patterns discovered in prior studies. For instance, our signature did not prominently feature portions of ventromedial prefrontal and orbitofrontal cortex (as identified by Canu *et al.*[39] and Du *et al.*[41]), nor did it feature portions of ventrolateral prefrontal (as identified by Ranasinghe *et al.*[29]), nor dorsolateral prefrontal cortex (as identified by Whitwell *et al.*,[20] Rabinovici *et al.*[40] and Du *et al.*[41]). Rather, in our signature, atrophy was relatively greater in dorsomedial prefrontal cortex; in dorsal and pregenual cingulate cortex; and in bilateral anterior temporal cortex—including the temporal pole and the anterior middle temporal gyrus and medial temporal lobe (Fig. 1).

From a circuit perspective, the specific networks affected in our bvFTD signature likely reflect the specific cognitive, behavioural and socio-emotional symptoms observed clinically. Consistent with prior reports, we found that portions of the salience network—including the fronto-insula and the dorsal anterior midcingulate cortex—were included in the signature. This is likely to account for impairments in detecting interoceptive and environmental salience in bvFTD patients.[16] In addition, involvement of the dorsal midcingulate node of the salience network may underlie motivational aspects of apathy[46,47]—a key diagnostic criterion in bvFTD.[24] Furthermore, the dorsal midcingulate region instantiates selected executive functions (e.g. response conflict, error monitoring, task switching),[48,49] which are commonly disrupted in bvFTD. However, our work also expands upon the networks considered to contribute to the cortical signature of bvFTD, helping to account for symptoms observed in this condition, which go beyond salience detection and the maintenance of homeostasis. In keeping with this, Shafiei *et al.*[11] found that, in a sample of genetic and sporadic bvFTD cases, atrophy was not statistically significant in the salience network. Instead, as in our study, atrophy was prominent in the limbic network and in the DMN.

The DMN was heavily represented in our bvFTD signature, contributing 46.3% to it. In particular, the dorsomedial prefrontal portion of the DMN contributed prominently to our signature. This region has consistently been implicated in taking the mental perspective of another person.[50-52] While not a core diagnostic criterion, impairments in this domain are reliably observed in bvFTD patients.[34,53,54] Moreover, while apathy is often associated with damage to the dorsal midcingulate node of the salience network, this bvFTD symptom has also been associated with atrophy in anterior portions of the DMN—specifically the rostral anterior cingulate and the ventromedial prefrontal cortex[46,47]; and other studies have implicated similar regions in AD patients with apathy.[55,56] Another DMN region included in the bvFTD atrophy signature was the anterior middle temporal gyrus. This region encompasses key portions of the language network in the left hemisphere[57] and social pragmatic and paralinguistic functions in the right hemisphere.[58] Its inclusion in the bvFTD signature could account for language and paralinguistic deficits often observed in bvFTD patients.[59]

Along similar lines, the prominence of atrophy in the limbic/semantic appraisal network in our bvFTD signature resonates with findings by Shafiei *et al.*[11] and Ranasinghe *et al.*[29] Specific symptoms common to bvFTD have been linked to dysfunction in regions of the limbic/semantic appraisal network. For example, behavioural disinhibition is a core bvFTD symptom[24] and among the most commonly observed clinically. Behavioural disinhibition is associated with lesions of orbitofrontal cortex, e.g. it is often associated with medial orbitofrontal damage resulting from traumatic brain injury.[60] Medial orbitofrontal atrophy has also been observed to correlate with disinhibition in FTD patients.[61,62] Second, this network is involved with coding the personal and hedonic value of semantic information, and bvFTD patients perform poorly on such tasks (e.g. identifying facial emotions).[63] Third, loss of empathy is another core criterion in bvFTD,[24] and the semantic appraisal (limbic) network—especially the right temporal pole and medial orbitofrontal cortex—has been discussed extensively by Rankin *et al.*[64,65] as central elements of the neural architecture associated with loss of empathy and egocentrism in bvFTD. Fourth, the prominence of right anterior temporal atrophy in our signature may also account for other symptoms routinely encountered in bvFTD patients, e.g. changes in eating behaviour and compulsive behaviour.[66,67]

With respect to the frontoparietal network, the involvement of this circuit in our signature also echoes known clinical deficits in bvFTD. The defining cognitive deficit in bvFTD is that of executive dysfunction,[24,68] and several executive domains are neurally instantiated in dorsolateral prefrontal and parietal regions of the frontoparietal network.[69,70] Prior investigations have linked atrophy in these network regions with executive dysfunction in bvFTD. For example, we previously demonstrated correlations between cortical thinning in the dorsolateral prefrontal cortex in patients with FTD/ALS and judgement/problem-solving scores on the Clinical Dementia Rating Scale.[71] Another study linked a measure of executive dysfunction (impaired sorting) in bvFTD patients with dorsolateral prefrontal atrophy.[72]

We also examined whether anatomic subtypes were embedded within our bvFTD signature. Hierarchical clustering demonstrated three major clusters of anatomic subtypes and these are similar to those discovered by other groups using clustering analyses.[20,29] For example, Whitwell *et al.*[20] performed a similar hierarchical agglomerative cluster analysis on a group of 66 individuals with bvFTD and found four anatomic subtypes—three of which overlap with the three clusters we report. More specifically: the 'frontotemporal subtype' detailed by this group topographically overlaps with our 'fronto-temporal cluster'; the 'temporofrontoparietal subtype' topographically overlaps with our 'fronto-temporo-parietal cluster'; and our 'anterior temporal-insular cluster' is topographically similar to the 'temporal dominant subtype' this group described. Ranasinghe *et al.*[29] used principal component and cluster analysis to identify distinct atrophy patterns in 90 bvFTD patients.

Their 'salience network-frontal/temporal' subgroup topographically overlaps with our 'fronto-temporal cluster', and their 'semantic appraisal network' subgroup anatomically resonates with our 'anterior temporal-insular' cluster.

Notably, our study, as well as these two prior studies, identified a single cluster that prominently included the anterior temporal lobe. This is consistent with the concept of a 'temporal variant'[66,73] of bvFTD, which heavily involves the temporal pole to the relative exclusion of frontal cortex. Of note, while the left temporal pole is characteristically atrophied in semantic variant primary progressive aphasia,[74] our findings highlight the frequency of the involvement of the right temporal pole in bvFTD. This resonates with the precept that right temporal predominant cases of bvFTD are traditionally under-recognized,[67] despite the finding that patients exhibit increasing bvFTD-like behavioural impairments as the right temporal pole becomes more involved.[75] Thus, our results again support the clinical observation that bvFTD can anatomically and phenotypically present as a syndrome preferentially affecting the temporal lobe.[67,76]

Our study is limited by the fact that we did not systematically obtain amyloid biomarkers on either sample. As such, it is possible that individuals with the behavioural/dysexecutive variant of AD were included. However, we consider it unlikely that a large portion of either sample harboured AD pathology, as all subjects met clinical criteria for bvFTD,[24] and individuals with the behavioural/dysexecutive variant of AD are less likely to fulfil the bvFTD criteria of disinhibition, hyperorality, loss of empathy and compulsive/repetitive behaviours.[77,78] Second, our analyses were limited to cortical structures. As such, our clustering approach was not able to identify putative clusters that may have included subcortical structures. For instance, Ranasinghe *et al.*[29] detailed a discrete subcortical cluster, which mostly involved the thalamus and striatum. Finally, the FTLD-NI sample did have a higher mean Clinical Dementia Rating (CDR) sum of boxes score than the MGH sample. As such, clinical severity in this sample was more advanced. The significance of this is tempered by the fact that our bvFTD signature was remarkably consistent across cohorts.

In conclusion, we identified a cortical atrophy signature of bvFTD that was remarkably similar across two independent patient cohorts. We then showed that topographically, networks affected by bvFTD are diverse, reflecting the phenotypic and anatomical diversity seen in patients who present with this behavioural-cognitive syndrome.[15] Future efforts could use this signature for diagnostic purposes. For example, quantitative algorithms that assess atrophy on clinically obtained MRIs could be used to better determine whether the regional atrophy pattern of a patient whose diagnosis is ambiguous matches that which is typical of bvFTD. In research contexts, this signature could be leveraged as a biomarker for early diagnosis. Finally, this work could provide a framework to predict how pathobiological changes spread across distant brain regions based on connectivity profiles.[11,79-81]

Acknowledgements

We thank our patients and family members for their participation, without which this work would not have been possible.

Funding

This study was supported by grants from the National Institute on Deafness and Other Communication Disorders (R01 DC014296) and the National Institute on Aging (R01 AG032306, P30 AG062241). This research was also supported by the National Institute of Biomedical Imaging and Bioengineering (P41EB015896). This work also involved the use of instrumentation supported by the National Institutes of Health Shared Instrumentation Grant Program and/or High-End Instrumentation Grant Program; specifically, grant number(s) S10RR021110, S10RR023043, S10RR023401. The content is solely the responsibility of the authors and does not necessarily represent the official views of the National Institutes of Health.

Competing interests

B.C.D. has served as a consultant for Acadia, Alector, Arkuda, Biogen, Denali, Eisai, Genentech, Lilly, Merck, Takeda, and Wave Lifesciences; he receives royalties from Cambridge University Press, Elsevier, and Oxford University Press. The other authors report no competing interests.

Supplementary material

Supplementary material is available at *Brain* online.

References

1. Dickerson BC, Bakkour A, Salat DH, *et al*. The cortical signature of Alzheimer's disease: Regionally specific cortical thinning relates to symptom severity in very mild to mild AD dementia and is detectable in asymptomatic amyloid-positive individuals. *Cereb Cortex*. 2009;19:497-510.
2. Dincer A, Gordon BA, Hari-Raj A, *et al*. Comparing cortical signatures of atrophy between late-onset and autosomal dominant Alzheimer disease. *Neuroimage Clin*. 2020;28:102491.
3. Oppedal K, Ferreira D, Cavallin L, *et al*. A signature pattern of cortical atrophy in dementia with Lewy bodies: A study on 333 patients from the European DLB consortium. *Alzheimers Dement*. 2019;15:400-409.
4. Seeley WW, Crawford RK, Zhou J, Miller BL, Greicius MD. Neurodegenerative diseases target large-scale human brain networks. *Neuron*. 2009;62:42-52.
5. Pievani M, de Haan W, Wu T, Seeley WW, Frisoni GB. Functional network disruption in the degenerative dementias. *Lancet Neurol*. 2011;10:829-843.
6. Palop JJ, Chin J, Mucke L. A network dysfunction perspective on neurodegenerative diseases. *Nature*. 2006;443:768-773.
7. Chhatwal JP, Schultz AP, Johnson KA, *et al*. Preferential degradation of cognitive networks differentiates Alzheimer's disease from ageing. *Brain*. 2018;141:1486-1500.
8. Zhou J, Greicius MD, Gennatas ED, *et al*. Divergent network connectivity changes in behavioural variant frontotemporal dementia and Alzheimer's disease. *Brain*. 2010;133(Pt 5):1352-1367.
9. Ng ASL, Wang J, Ng KK, *et al*. Distinct network topology in Alzheimer's disease and behavioral variant frontotemporal dementia. *Alzheimers Res Ther*. 2021;13:13.
10. Hafkemeijer A, Moller C, Dopper EG, *et al*. Differences in structural covariance brain networks between behavioral variant frontotemporal dementia and Alzheimer's disease. *Hum Brain Mapp*. 2016;37:978-988.
11. Shafiei G, Bazinet V, Dadar M, *et al*. Network structure and transcriptomic vulnerability shape atrophy in frontotemporal dementia. *Brain*. 2023;146:321–3336.
12. Buckner RL, Sepulcre J, Talukdar T, *et al*. Cortical hubs revealed by intrinsic functional connectivity: Mapping, assessment of

stability, and relation to Alzheimer's disease. *J Neurosci*. 2009;29: 1860-1873.
13. Jin D, Wang P, Zalesky A, *et al*. Grab-AD: Generalizability and reproducibility of altered brain activity and diagnostic classification in Alzheimer's disease. *Hum Brain Mapp*. 2020;41:3379-3391.
14. Dickerson BC, Brickhouse M, McGinnis S, Wolk DA. Alzheimer's disease: The influence of age on clinical heterogeneity through the human brain connectome. *Alzheimers Dement (Amst)*. 2017;6: 122-135.
15. Lehmann M, Madison CM, Ghosh PM, *et al*. Intrinsic connectivity networks in healthy subjects explain clinical variability in Alzheimer's disease. *Proc Natl Acad Sci U S A*. 2013;110: 11606-11611.
16. Seeley WW. The salience network: A neural system for perceiving and responding to homeostatic demands. *J Neurosci*. 2019;39: 9878-9882.
17. Sturm VE, Brown JA, Hua AY, *et al*. Network architecture underlying basal autonomic outflow: Evidence from frontotemporal dementia. *J Neurosci*. 2018;38:8943-8955.
18. Carr AR, Jimenez EE, Thompson PM, Mendez MF. Frontotemporal asymmetry in socioemotional behavior: A pilot study in frontotemporal dementia. *Soc Neurosci*. 2020;15:15-24.
19. Kamminga J, Kumfor F, Burrell JR, Piguet O, Hodges JR, Irish M. Differentiating between right-lateralised semantic dementia and behavioural-variant frontotemporal dementia: An examination of clinical characteristics and emotion processing. *J Neurol Neurosurg Psychiatry*. 2015;86:1082-1088.
20. Whitwell JL, Przybelski SA, Weigand SD, *et al*. Distinct anatomical subtypes of the behavioural variant of frontotemporal dementia: A cluster analysis study. *Brain*. 2009;132(Pt 11): 2932-2946.
21. Yeo BT, Krienen FM, Sepulcre J, *et al*. The organization of the human cerebral cortex estimated by intrinsic functional connectivity. *J Neurophysiol*. 2011;106:1125-1165.
22. Sapolsky D, Domoto-Reilly K, Dickerson BC. Use of the progressive aphasia severity scale (PASS) in monitoring speech and language status in PPA. *Aphasiology*. 2014;28(8–9):993-1003.
23. Sapolsky D, Domoto-Reilly K, Negreira A, Brickhouse M, McGinnis SM, Dickerson BC. Monitoring progression of primary progressive aphasia: Current approaches and future directions. *Neurodegener Dis Manag*. 2011;1:43-55.
24. Rascovsky K, Hodges JR, Knopman D, *et al*. Sensitivity of revised diagnostic criteria for the behavioural variant of frontotemporal dementia. *Brain*. 2011;134(Pt 9):2456-2477.
25. Putcha D, Eckbo R, Katsumi Y, Dickerson BC, Touroutoglou A, Collins JA. Tau and the fractionated default mode network in atypical Alzheimer's disease. *Brain Commun*. 2022;4:fcac055.
26. Katsumi Y, Putcha D, Eckbo R, *et al*. Anterior dorsal attention network tau drives visual attention deficits in posterior cortical atrophy. *Brain*. 2023;146:295–2306.
27. Cohen AL, Fair DA, Dosenbach NU, *et al*. Defining functional areas in individual human brains using resting functional connectivity MRI. *Neuroimage*. 2008;41:45-57.
28. Bakkour A, Morris JC, Wolk DA, Dickerson BC. The effects of aging and Alzheimer's disease on cerebral cortical anatomy: Specificity and differential relationships with cognition. *Neuroimage*. 2013;76:332-344.
29. Ranasinghe KG, Rankin KP, Pressman PS, *et al*. Distinct subtypes of behavioral variant frontotemporal dementia based on patterns of network degeneration. *JAMA Neurol*. 2016;73:1078-1088.
30. Ranasinghe KG, Toller G, Cobigo Y, *et al*. Computationally derived anatomic subtypes of behavioral variant frontotemporal dementia show temporal stability and divergent patterns of longitudinal atrophy. *Alzheimers Dement (Amst)*. 2021;13:e12183.
31. Vuksanovic V, Staff RT, Morson S, *et al*. Degeneration of basal and limbic networks is a core feature of behavioural variant frontotemporal dementia. *Brain Commun*. 2021;3:fcab241.
32. Abraham A, Pedregosa F, Eickenberg M, *et al*. Machine learning for neuroimaging with scikit-learn. *Front Neuroinform*. 2014;8:14.
33. Young AL, Marinescu RV, Oxtoby NP, *et al*. Uncovering the heterogeneity and temporal complexity of neurodegenerative diseases with subtype and stage inference. *Nat Commun*. 2018;9: 4273.
34. Eslinger PJ, Moore P, Anderson C, Grossman M. Social cognition, executive functioning, and neuroimaging correlates of empathic deficits in frontotemporal dementia. *J Neuropsychiatry Clin Neurosci*. 2011;23:74-82.
35. Pan PL, Song W, Yang J, *et al*. Gray matter atrophy in behavioral variant frontotemporal dementia: A meta-analysis of voxel-based morphometry studies. *Dement Geriatr Cogn Disord*. 2012; 33(2–3):141-148.
36. Pereira JM, Williams GB, Acosta-Cabronero J, *et al*. Atrophy patterns in histologic vs clinical groupings of frontotemporal lobar degeneration. *Neurology*. 2009;72:1653-1660.
37. McMillan CT, Avants BB, Cook P, Ungar L, Trojanowski JQ, Grossman M. The power of neuroimaging biomarkers for screening frontotemporal dementia. *Hum Brain Mapp*. 2014;35: 4827-4840.
38. Moller C, Pijnenburg YA, van der Flier WM, *et al*. Alzheimer Disease and behavioral variant frontotemporal dementia: Automatic classification based on cortical atrophy for single-subject diagnosis. *Radiology*. 2016;279:838-848.
39. Canu E, Agosta F, Mandic-Stojmenovic G, *et al*. Multiparametric MRI to distinguish early onset Alzheimer's disease and behavioural variant of frontotemporal dementia. *Neuroimage Clin*. 2017;15:428-438.
40. Rabinovici GD, Seeley WW, Kim EJ, *et al*. Distinct MRI atrophy patterns in autopsy-proven Alzheimer's disease and frontotemporal lobar degeneration. *Am J Alzheimers Dis Other Demen*. 2008;22:474-488.
41. Du AT, Schuff N, Kramer JH, *et al*. Different regional patterns of cortical thinning in Alzheimer's disease and frontotemporal dementia. *Brain*. 2006;130(Pt 4):1159-1166.
42. Alexander L, Wood CM, Gaskin PLR, *et al*. Over-activation of primate subgenual cingulate cortex enhances the cardiovascular, behavioral and neural responses to threat. *Nat Commun*. 2020; 11:5386.
43. Weigand A, Horn A, Caballero R, *et al*. Prospective validation that subgenual connectivity predicts antidepressant efficacy of transcranial magnetic stimulation sites. *Biol Psychiatry*. 2018;84:28-37.
44. Hadas I, Sun Y, Lioumis P, *et al*. Association of repetitive transcranial magnetic stimulation treatment with subgenual cingulate hyperactivity in patients with Major depressive disorder: A secondary analysis of a randomized clinical trial. *JAMA Netw Open*. 2019;2:e195578.
45. Siddiqi SH, Schaper F, Horn A, *et al*. Brain stimulation and brain lesions converge on common causal circuits in neuropsychiatric disease. *Nat Hum Behav*. 2021;5:1707.
46. Massimo L, Powers JP, Evans LK, *et al*. Apathy in frontotemporal degeneration: Neuroanatomical evidence of impaired goal-directed behavior. *Front Hum Neurosci*. 2015;9:611.
47. Lansdall CJ, Coyle-Gilchrist ITS, Jones PS, *et al*. Apathy and impulsivity in frontotemporal lobar degeneration syndromes. *Brain*. 2017;140:1792-1807.
48. Menon V, Uddin LQ. Saliency, switching, attention and control: A network model of insula function. *Brain Struct Funct*. 2010; 214(5–6):655-667.

49. Uddin LQ. Salience processing and insular cortical function and dysfunction. *Nat Rev Neurosci*. 2015;16:55-61.
50. Buckner RL, DiNicola LM. The brain's default network: Updated anatomy, physiology and evolving insights. *Nat Rev Neurosci*. 2019;20:593-608.
51. DiNicola LM, Braga RM, Buckner RL. Parallel distributed networks dissociate episodic and social functions within the individual. *J Neurophysiol*. 2020;123:1144-1179.
52. van Veluw SJ, Chance SA. Differentiating between self and others: An ALE meta-analysis of fMRI studies of self-recognition and theory of mind. *Brain Imaging Behav*. 2014;8:24-38.
53. Shany-Ur T, Poorzand P, Grossman SN, *et al*. Comprehension of insincere communication in neurodegenerative disease: Lies, sarcasm, and theory of mind. *Cortex*. 2012;48:1329-1341.
54. Bickart KC, Brickhouse M, Negreira A, Sapolsky D, Barrett LF, Dickerson BC. Atrophy in distinct corticolimbic networks in frontotemporal dementia relates to social impairments measured using the social impairment rating scale. *J Neurol Neurosurg Psychiatry*. 2014;85:438-448.
55. Bruen PD, McGeown WJ, Shanks MF, Venneri A. Neuroanatomical correlates of neuropsychiatric symptoms in Alzheimer's disease. *Brain*. 2008;131(Pt 9):2455-2463.
56. Marshall GA, Monserratt L, Harwood D, Mandelkern M, Cummings JL, Sultzer DL. Positron emission tomography metabolic correlates of apathy in Alzheimer disease. *Arch Neurol*. 2007;64:1015-1020.
57. Fedorenko E, Thompson-Schill SL. Reworking the language network. *Trends Cogn Sci*. 2014;18:120-126.
58. Mendez MF, Carr AR, Paholpak P. Psychotic-Like speech in frontotemporal dementia. *J Neuropsychiatry Clin Neurosci*. 2017;29:183-185.
59. Hardy CJ, Buckley AH, Downey LE, *et al*. The language profile of behavioral variant frontotemporal dementia. *J Alzheimers Dis*. 2016;50:359-371.
60. Knutson KM, Dal Monte O, Schintu S, *et al*. Areas of brain damage underlying increased reports of behavioral disinhibition. *J Neuropsychiatry Clin Neurosci*. 2015;27:193-198.
61. Massimo L, Powers C, Moore P, *et al*. Neuroanatomy of apathy and disinhibition in frontotemporal lobar degeneration. *Dement Geriatr Cogn Disord*. 2009;27:96-104.
62. Viskontas IV, Possin KL, Miller BL. Symptoms of frontotemporal dementia provide insights into orbitofrontal cortex function and social behavior. *Ann N Y Acad Sci*. 2007;1121:528-545.
63. Yang WFZ, Toller G, Shdo S, *et al*. Resting functional connectivity in the semantic appraisal network predicts accuracy of emotion identification. *Neuroimage Clin*. 2021;31:102755.
64. Rankin KP, Gorno-Tempini ML, Allison SC, *et al*. Structural anatomy of empathy in neurodegenerative disease. *Brain*. 2006;129(Pt 11):2945-2956.
65. Rankin KP. Measuring behavior and social cognition in FTLD. *Adv Exp Med Biol*. 2021;1281:51-65.
66. Seeley WW, Bauer AM, Miller BL, *et al*. The natural history of temporal variant frontotemporal dementia. *Neurology*. 2005;64:1384-1390.
67. Josephs KA, Whitwell JL, Knopman DS, *et al*. Two distinct subtypes of right temporal variant frontotemporal dementia. *Neurology*. 2009;73:1443-1450.
68. Libon DJ, Xie SX, Moore P, *et al*. Patterns of neuropsychological impairment in frontotemporal dementia. *Neurology*. 2007;68:369-375.
69. Reineberg AE, Banich MT. Functional connectivity at rest is sensitive to individual differences in executive function: A network analysis. *Hum Brain Mapp*. 2016;37:2959-2975.
70. Menon V, D'Esposito M. The role of PFC networks in cognitive control and executive function. *Neuropsychopharmacology*. 2022;47:90–103.
71. Ratti E, Domoto-Reilly K, Caso C, *et al*. Regional prefrontal cortical atrophy predicts specific cognitive-behavioral symptoms in ALS-FTD. *Brain Imaging Behav*. 2021;15:2540–22551.
72. Huey ED, Goveia EN, Paviol S, *et al*. Executive dysfunction in frontotemporal dementia and corticobasal syndrome. *Neurology*. 2009;72:453-459.
73. Thompson SA, Patterson K, Hodges JR. Left/right asymmetry of atrophy in semantic dementia: Behavioral-cognitive implications. *Neurology*. 2003;61:1196-1203.
74. Collins JA, Montal V, Hochberg D, *et al*. Focal temporal pole atrophy and network degeneration in semantic variant primary progressive aphasia. *Brain*. 2017;140:457-471.
75. Eldaief MC, Perez DL, Quimby M, *et al*. Atrophy in distinct corticolimbic networks subserving socioaffective behavior in semantic variant primary progressive aphasia. *Dement Geriatr Cogn Disord*. 2020;49:589-597.
76. Younes K, Borghesani V, Montembeault M, *et al*. Right temporal lobe and socioemotional semantics: Semantic behavioural variant frontotemporal dementia. *Brain*. 2022;145:4080–44096.
77. Ossenkoppele R, Pijnenburg YA, Perry DC, *et al*. The behavioural/dysexecutive variant of Alzheimer's disease: Clinical, neuroimaging and pathological features. *Brain*. 2015;138(Pt 9):2732-2749.
78. Barker MS, Gottesman RT, Manoochehri M, *et al*. Proposed research criteria for prodromal behavioural variant frontotemporal dementia. *Brain*. 2022;145:1079-1097.
79. Jucker M, Walker LC. Propagation and spread of pathogenic protein assemblies in neurodegenerative diseases. *Nat Neurosci*. 2018;21:1341-1349.
80. Zhou J, Gennatas ED, Kramer JH, Miller BL, Seeley WW. Predicting regional neurodegeneration from the healthy brain functional connectome. *Neuron*. 2012;73:1216-1227.
81. Brown JA, Deng J, Neuhaus J, *et al*. Patient-Tailored, connectivity-based forecasts of spreading brain atrophy. *Neuron*. 2019;104:856-868.e5.